https://doi.org/10.5194/egusphere-2023-3123
Preprint. Discussion started: 24 January 2024

Miocene evolution of the NW Zagros foreland basin reflects SE-ward propagating tear of the Neotethys slab

Renas I. Koshnaw[1, a], Jonas Kley[1], Fritz Schlunegger[2]

[1]Department of Structural Geology and Geodynamics, Geoscience Center, University of Goettingen, Goldschmidtstrasse 3, 37077 Göttingen, Germany
[2]Institute of Geological Sciences, University of Bern, 3012 Bern, Switzerland

Correspondence to: Renas I. Koshnaw (renas.i.koshnaw@gmail.com)

Abstract. Tectonic processes resulting from solid Earth dynamics control uplift and generate sediment accommodation space via subsidence. Unraveling the mechanism of basin subsidence elucidates the link between deep Earth and Surface processes. The NW Zagros fold-thrust belt results from the Cenozoic convergence and subsequent collision between the Arabian and Eurasian plates. The associated Neogene foreland basin includes ~4 km of syntectonic nonmarine clastic sediments, suggesting a strongly subsiding basin inconsistent with the adjacent topographic load. To explain such discrepancy, we assessed basin subsidence with respect to the effect of surface load and dynamic topography. The isopach map of the Fatha Formation during the middle Miocene displays a longitudinal depocenter aligned with the orogenic trend. In contrast, the maps of the Injana Formation and Mukdadiya Formation during the late Miocene illustrate a focused depocenter in the southern region of the basin. The rapid subsidence in the south during the late Miocene was coeval with the Afar plume flow northward beyond the Arabia-Eurasia suture zone in the northwestern segment of the Zagros belt. Based on isopach maps, subsidence curves, and reconstructions of flexural profiles, supported by Bouguer anomaly data and maps of dynamic topography and seismic tomography, we argue for a two-stage basin evolution. The Zagros foreland basin subsided due to the load of the surface and the subducting slab during the early-middle Miocene and was later affected by the Neotethys horizontal slab tear propagation during the late Miocene. This tear propagation was associated with a northward mantle flow above the detached segment in the NW and a focused slab pull on the attached portion of the slab in the SE.

1 Introduction

Formation of fold-thrust belts and the evolution of adjoining basins may take tens of millions of years and involves large-scale processes such as deformation, magmatism, metamorphism, uplift, and subsidence that are collectively coupled with mantle flow and lithosphere dynamics (Royden, 1993; Allen and Allen, 2013). At convergent plate boundaries, accommodation space is created by the flexural bending of the foreland plate due to surface and slab loading (Schlunegger and Kissling, 2022). In addition, the history of such a basin could be influenced by mantle flow and the evolution of dynamic

https://doi.org/10.5194/egusphere-2023-3123
Preprint. Discussion started: 24 January 2024

topography (Dávila and Lithgow-Bertelloni, 2013; Jolivet et al., 2015; Heller and Liu, 2016). During orogenesis, continents converge through two main mechanisms to form a mountain belt and create a foreland basin: slab-pull orogeny, driven mainly by the weight of the downgoing slab, and mantle orogeny, driven by shear traction along the bottom of the plate as mantle flows (Conrad and Lithgow-Bertelloni, 2004; Schlunegger and Kissling, 2015; Royden and Faccenna, 2018; Faccenna et al., 2021). In convergent plate boundaries, particularly in continent collisional zones, a slab breakoff may occur. The slab breakoff process affects the orogeny, the development of topography and surface mass flux (Sinclair, 1997), the foreland basin formation, and the flow of mantle materials at depth (Kissling and Schlunegger, 2018; Vanderhaeghe, 2012). Slab breakoff is considered to occur when the buoyant continental lithosphere starts to enter the subduction channel. This results in tensional forces between the subducted oceanic and continental parts of the plate, with the consequence that the denser subducting oceanic lithosphere detaches from the lighter continental counterpart and sinks, thereby triggering magmatism, uplift, and the exhumation of metamorphic rocks (Davies and von Blanckenburg, 1995). The dense oceanic slab separating from its more buoyant continental counterpart is thought to involve a sequence of processes, including slab necking, tearing and detachment, and eventually slab breakoff (complete detachment of slab) (Kundu and Santosh, 2011). Even though these processes take place at depths of hundreds of kilometers and have not been fully understood (e.g., Niu, 2017; Garzanti et al., 2018), potential surficial consequences through time and space could be constrained by geologic records and numerical models (Sinclair, 1997; Duretz and Gerya, 2013; Jolivet et al., 2015; Boutoux et al., 2021; van Hunen and Allen, 2011; Garefalakis and Schlunegger, 2018). Furthermore, global tomography and the results of numerical models highlight that these processes occur in 3D, and envisioning them in 2D may not provide enough insight (Hafkenscheid et al., 2006; van Hunen and Allen, 2011; Balázs et al., 2021). As slab breakoff occurs along the continental suture zone, essential changes in the force balance are expected to occur, with the consequence of measurable geologic processes on the surface such as uplift, subsidence, and an increase in mantle-influenced magmatism (Wortel and Spakman, 2000).

Unlike along the subduction boundary of the Americas, a delamination of the downgoing Neotethys oceanic slab has been suggested to occur along the collisional boundary of Eurasia beneath the Alps, the Zagros, and the Himalaya. Among these belts, the Zagros orogen is the youngest and the least deformed belt and has a relatively complete and well–preserved rock record (Hatzfeld and Molnar, 2010). Because the Arabia–Eurasia continental collision commenced in the area of the NW Zagros fold-thrust belt (McQuarrie and Hinsbergen, 2013), this segment of the mountain belt and the related foreland basin are particularly interesting for inferring the controls on the construction of the orogen and the adjacent foreland basin (Fig. 1). Furthermore, the documented along–strike variations in geological properties near the surface (e.g., the timing of the Main Zagros fault activation, age of exposed rocks, foreland basin accommodation) and at depth (thermal lithospheric thickness, age, chemistry of the late Miocene magmatism, and slow versus fast seismic velocity in the upper mantle) render this orogen an ideal laboratory to analyze the geological record of time-transgressive orogenesis.

https://doi.org/10.5194/egusphere-2023-3123
Preprint. Discussion started: 24 January 2024

This research in the NW Zagros belt in the Kurdistan region of Iraq aims to constrain the mechanisms by which the Zagros basin evolved in relation to geodynamic processes such as slab breakoff and mantle dynamics. For this purpose, we generated new isopach maps and subsidence curves and evaluated the flexural effect of the Neogene Zagros topography. Furthermore, we synthesized regional Bouguer gravity anomaly and dynamic topography maps as well as teleseismic tomographic data and the magmatic record in the Middle East (Amaru, 2007; Hall and Spakman, 2015; Ball et al., 2021) to guide interpretations and analyze the occurrence of possible surface signals attributable to slab breakoff beneath the orogen.

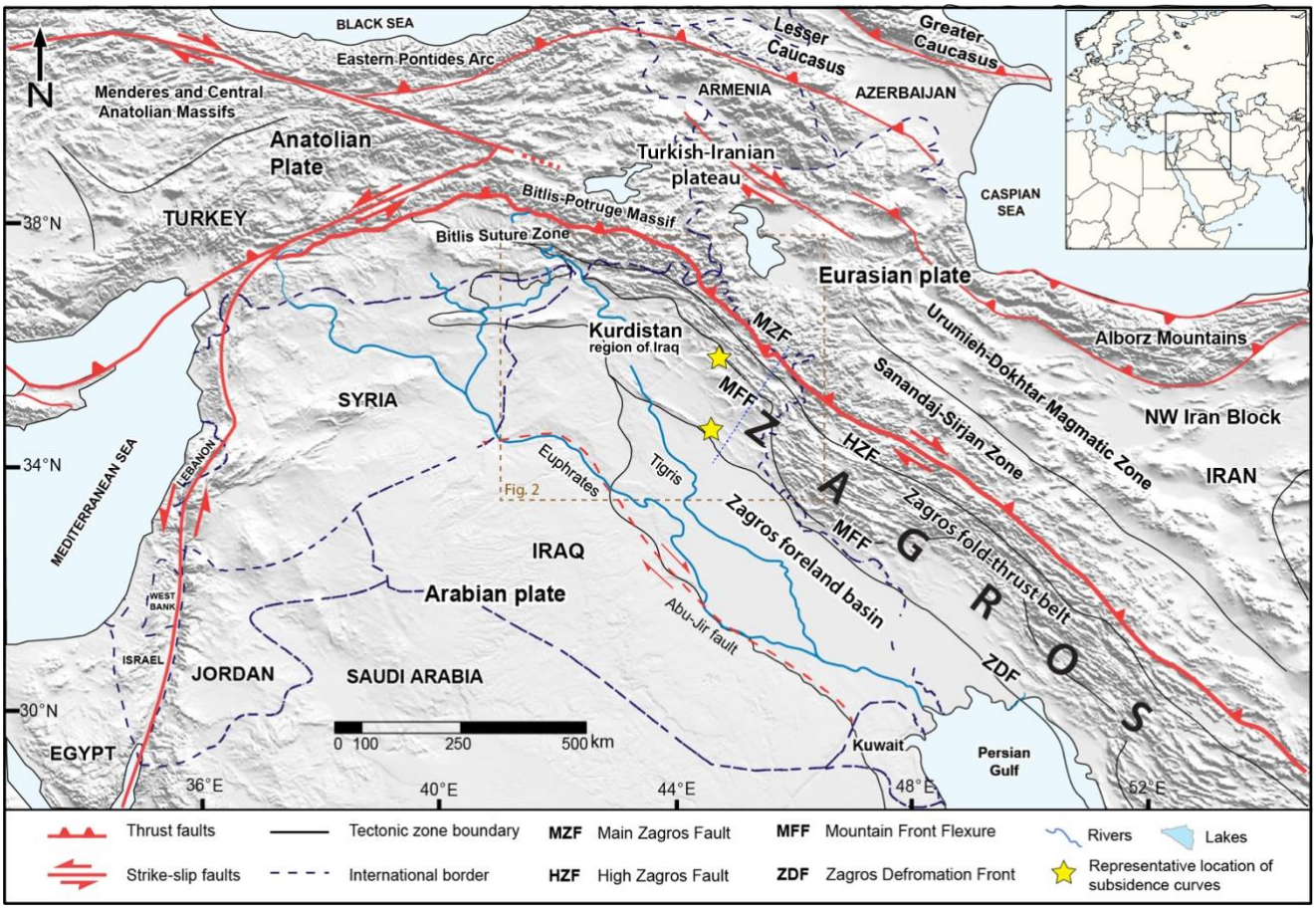

Figure 1: Tectonic map of the Middle East showing the main structural features, tectonic plates, and the study area in the northwestern segment of the Zagros fold-thrust belt and foreland basin. The dashed brown box represents the study area. The shaded relief map was generated from the ASTER Global Digital Elevation Map (2011) data set (asterweb.jpl.nasa.gov/gdem.asp).

2 Tectonostratigraphic context

After the complete subduction of the Neotethys oceanic slab beneath the Eurasian continental plate, the continental part of the Arabian plate started to enter the subduction zone and thus collided with the Eurasian plate during the Oligocene, (Allen

https://doi.org/10.5194/egusphere-2023-3123
Preprint. Discussion started: 24 January 2024

and Armstrong, 2008; Koshnaw et al., 2019, 2021). Consequently, the foreland basin situated on the Arabian plate shifted from being underfilled with primarily deeper to shallow marine deposits (obduction-related proto-Zagros) to filled and overfilled with mostly nonmarine clastic deposits (Neogene Zagros) (Fg. 2). Both suites are separated by an Oligocene unconformity, particularly in the hinterland. This is because, before the Neogene, the proto-Zagros fold-thrust belt was already in place as highlands in the northeastern frontiers of Arabia. Along the Arabia–Eurasia suture zone, clastic and carbonate rocks of the Red Beds Series (RBS) were deposited in an intermontane basin on the Arabian plate, situated immediately below the Main Zagros fault (MZF). The RBD strata show an angular unconformity with the older deformed strata from the highlands of the proto-Zagros. The clastic units of the Merga and Suwais Groups from the RBS contain provenance signatures from Eurasia and the beds from the lower contact have a maximum depositional age of ~26 Ma (Koshnaw et al., 2019). The RBS consists of the nonmarine clastic Suwais Group, unconformably overlain by the shallow marine carbonate rocks of the Govanda Formation and the nonmarine clastic Merga Group on top. These units of the RBS were overthrusted by the allochthonous thrust sheets of the Walash–Naopurdan–Kamyaran (WNK) and ophiolitic terranes.

Away from the suture zone, the present-day NW Zagros Neogene foreland basin includes a ~3-4 km thick succession that consists of the mixed clastic–carbonate–evaporite beds of the Fatha Formation and the clastics of the Injana, Mukdadiya, and Bai–Hasan Formations (Fig. 2). These formations constitute classical foreland basin components with an upward coarsening and thickening succession (DeCelles, 2012). Data on detritus provenance and stratigraphic correlations in the NW Zagros belt indicate that the post–Oligocene foreland basin was a contiguous basin up to the latest Miocene. Afterward, the basin was structurally partitioned due to the out-of-sequence growth of the mountain front (Koshnaw et al., 2020a).

During the middle Miocene, the Fatha Formation was deposited in a lagoonal environment on the Arabian plate, fringing the NW-SE Zagros fold-thrust belt. This formation is primarily evaporitic in the depocenter, consisting of alternating beds of marls, limestones, and gypsum, whereas marls, limestones, mudstones, and fine- to medium-grained sandstones predominate toward the basin periphery (Shawkat and Tucker, 1978). In the NW Zagros belt, the thickness of the Fatha Formation increases from the margin (c. 300 m) to the center (c. 600 m) of the basin (Dunnington, 1958; Koshnaw et al., 2020b). Provenance evidence based on detrital zircon U-Pb ages shows that the sandstone component of the Fatha Formation was delivered mainly from the Paleozoic rocks in the N and Paleogene rocks in the NE (Koshnaw et al., 2020b). Being an incompetent layer in the stratigraphic column, the Fatha Formation became a décollement layer, detaching the post-Fatha units from the underlying stratigraphic units and leading to the genesis of shallow structures in the NW Zagros belt.

In the late Miocene, the clastic Injana Formation was deposited, marking a fundamental change in the depositional environment from marine to nonmarine. During this time, clastic sediments were delivered to the basin by an orogen-parallel fluvial system, transporting fine-grained sediments through meandering and low-sinuosity channel belts (Koshnaw et al., 2020b). The thickness varies significantly from the NW to the SE, increasing from ~300 m to ~1600 m. Detrital zircon U-Pb

https://doi.org/10.5194/egusphere-2023-3123
Preprint. Discussion started: 24 January 2024

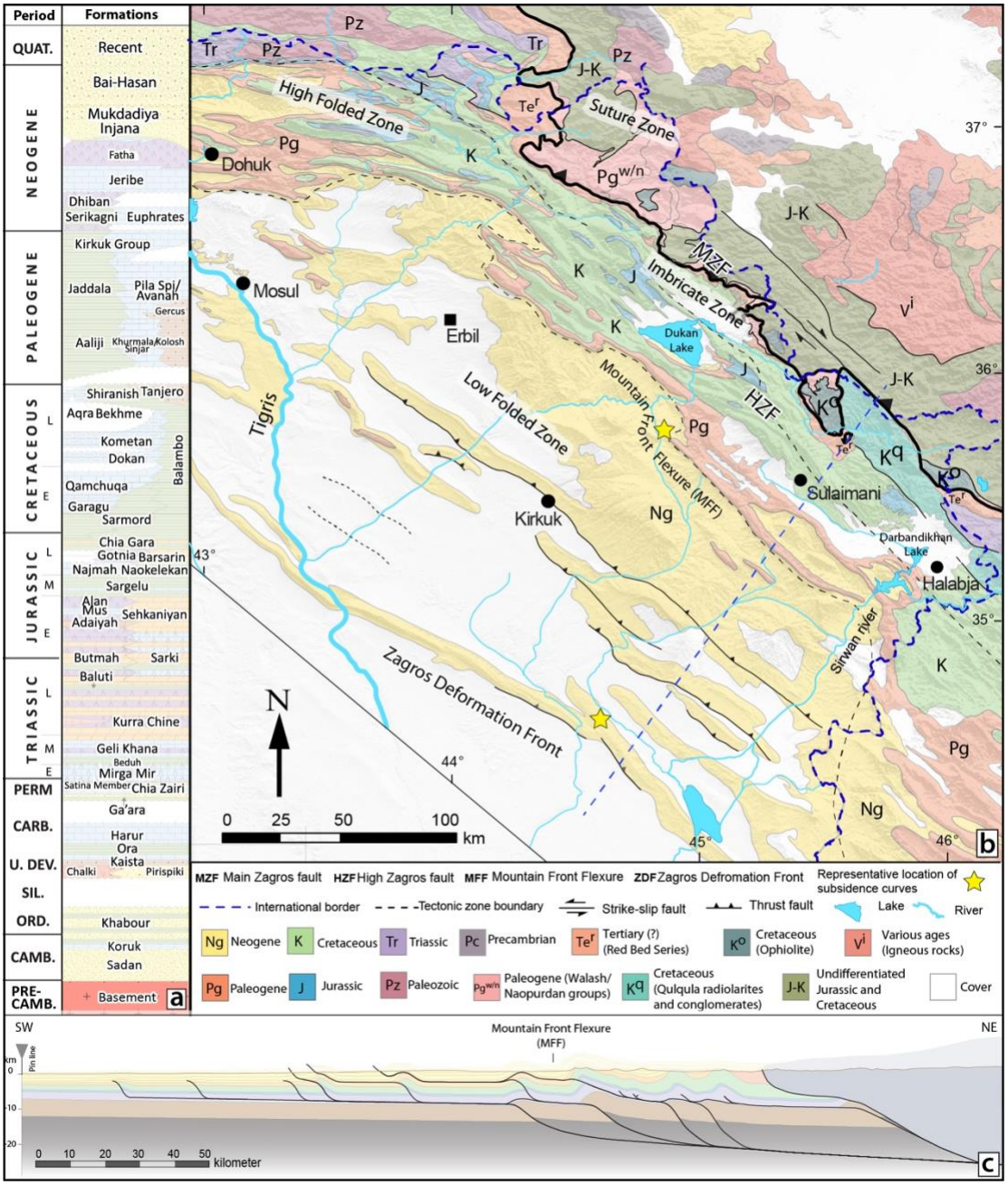

Figure 2: (a) Chronostratigraphic column showing the major rock units in the NW Zagros belt, including the Neogene Zagros foreland basin deposits (Fatha, Injana, Mukdadiya, and Bai-Hasan Formations). After English et al. (2015). (b) Geologic map of the NW Zagros fold-thrust belt and foreland basin exhibiting the spatial distribution of key rock exposures and structural subdivisions (Koshnaw et al., 2020a), (c) Balanced cross-section across the NW Zagros fold-thrust belt and foreland basin (see the geologic map for location) highlighting the key subsurface faults and fold-thrust belt geometry (Koshnaw et al., 2020a).

https://doi.org/10.5194/egusphere-2023-3123
Preprint. Discussion started: 24 January 2024

ages signature and apatite (U-Th)/He data imply that the deposition of the Injana Formation occurred contemporaneously with the uplift of the northern terranes beyond the Arabia–Eurasia suture zone, and with the reactivation of the Main Zagros fault along the suture zone with a right-lateral strike-slip component (Koshnaw et al., 2020a).

The Mukdadiya Formation was deposited throughout the latest Miocene, with sediments mainly derived from northeastern terranes and supplied to the basin by straight, high-energy transverse fluvial systems. The thickness of the Mukdadiya Formation varies from ~300 to ~1,000 m. This shift in the fluvial style between the Injana and Mukdadiya Formations occurred simultaneously with the advance of the deformation front into the foreland as documented by growth strata. By the Pliocene, the basin was structurally compartmentalized, with basement-involved thrusting resulting in the formation of the mountain front flexure (MFF) (Fig. 2). During this time, the Bai-Hasan Formation was deposited, consisting mainly of conglomeratic beds at proximal sites and mudstone layers in the distal parts. In proximal positions, the sediments of this formation were likely deposited by alluvial sheet floods during ephemeral runoff, whereas in the distal parts, discharge occurred in alluvial channels that were bordered by floodplains.

3 Methods

Isopach maps were constructed for the Fatha, Injana, and Mukdadiya Formations, and we also created a map that considers the ensemble of these units. These maps were drawn in *ArcGIS Map* based on published stratigraphic thicknesses, well data, estimated thickness from geological maps, and seismic profiles. The source of each data point (Injana Formation: 42; Mukdadiya Formation: 33) is available in the supplementary data section (S1). For the Fatha Formation, the construction of the isopach map was guided by the published contour lines of Dunnington (1958). The other maps were drafted solely relying on the control points.

Subsidence curves derived from backstripping curves were established for two localities: one in the north adjacent to the MFF, near the hinterland, and another one in the south in the vicinity of the depocenter. This was accomplished using the method described in Angevine et al. (1990). Data on thicknesses, lithologies, densities, porosities, compaction coefficients, and water depth were compiled from Al-Naqib (1959), Al-Sheikhly et al. (2015), Sachsenhofer et al. (2015), Koshnaw et al. (2020b). The data used for creating the subsidence curves are available in the supplementary data section (S2).

https://doi.org/10.5194/egusphere-2023-3123
Preprint. Discussion started: 24 January 2024

The flexural response of the foreland plate to loading was calculated using the concept of a broken beam overlying a fluid substratum using *Flex2D* (v. 5.2: Cardozo, 2021), which employs solutions based on Hetenyi (1946) and Bodine (1981). We used variable elastic thicknesses below the tectonic load (30-50 km from the MZF to the MFF) and a constant elastic thickness below the sedimentary load (50 km). The elastic thickness variation was estimated based on Saura et al. (2015) and Pirouz et al. (2017). A balanced cross-section (Koshnaw et al., 2020a) across the NW Zagros fold-thrust belt and foreland basin was used as a base for the modeling. Loads were measured above a horizontal reference line projected mountainward from the bottom of the undeformed Fatha Formation in the foreland (pin line location). For the purpose of flexural modeling, the trace of the balanced cross-section was extended to western Iraq, where the Fatha Formation and older rock units are exposed. Input data and used parameters can be found in the supplementary data section (S3).

Data for constructing the Bouguer gravity anomaly map was obtained from the Earth Gravitational Model (EGM2008: Pavlis et al., 2008), which has a spatial resolution of 2.5 arc-minute by 2.5 arc-minute (~3.7 km at latitude N36°). The dynamic topography map was digitized from Craig et al. (2011: Fig. 15d), which was calculated from the free-air gravity anomaly. Crystallization ages of igneous rocks with mantle origin were taken from Ball et al. (2021) to assess magmatic activity. Tomographic maps and profiles are based on the global P-wave velocity anomaly model UU-P07 by Amaru (2007) and Hall and Spakman (2015) and processed using the web-based tool *SubMachine* (Hosseini et al., 2018). The spatial resolution of the tomographic image varies depending on depth: 50 km from the base of the crust down to 410 km and then 65 km down to 660 km (Hall and Spakman, 2015). P-wave velocity anomalies are indicated relative to the reference model ak135 of Kennett et al. (1995).

4 Results

4.1 Isopach maps

The isopach maps for the Fatha, Injana, and Mukdadiya Formations display variations in the basin architecture and illustrate an overall southeastward-directed thickness increase (Fig. 3). The map for the Fatha Formation is noticeably different from those of the Injana and Mukdadiya Formations in the sense that the isopach pattern of the Fatha unit suggests a depocenter

https://doi.org/10.5194/egusphere-2023-3123
Preprint. Discussion started: 24 January 2024

with c. 600 m thick sediments parallel to the NW-SE trend of the Zagros fold-thrust belt. By contrast, the thicknesses of the overlying Injana and Mukdadiya Formations point to a southward shift in the basin axis, which also rotated to a more N–S orientation. The thickness of the Fatha, Injana, and Mukdadiya Formations collectively reaches ~3000 m in the southern segment of the study area.

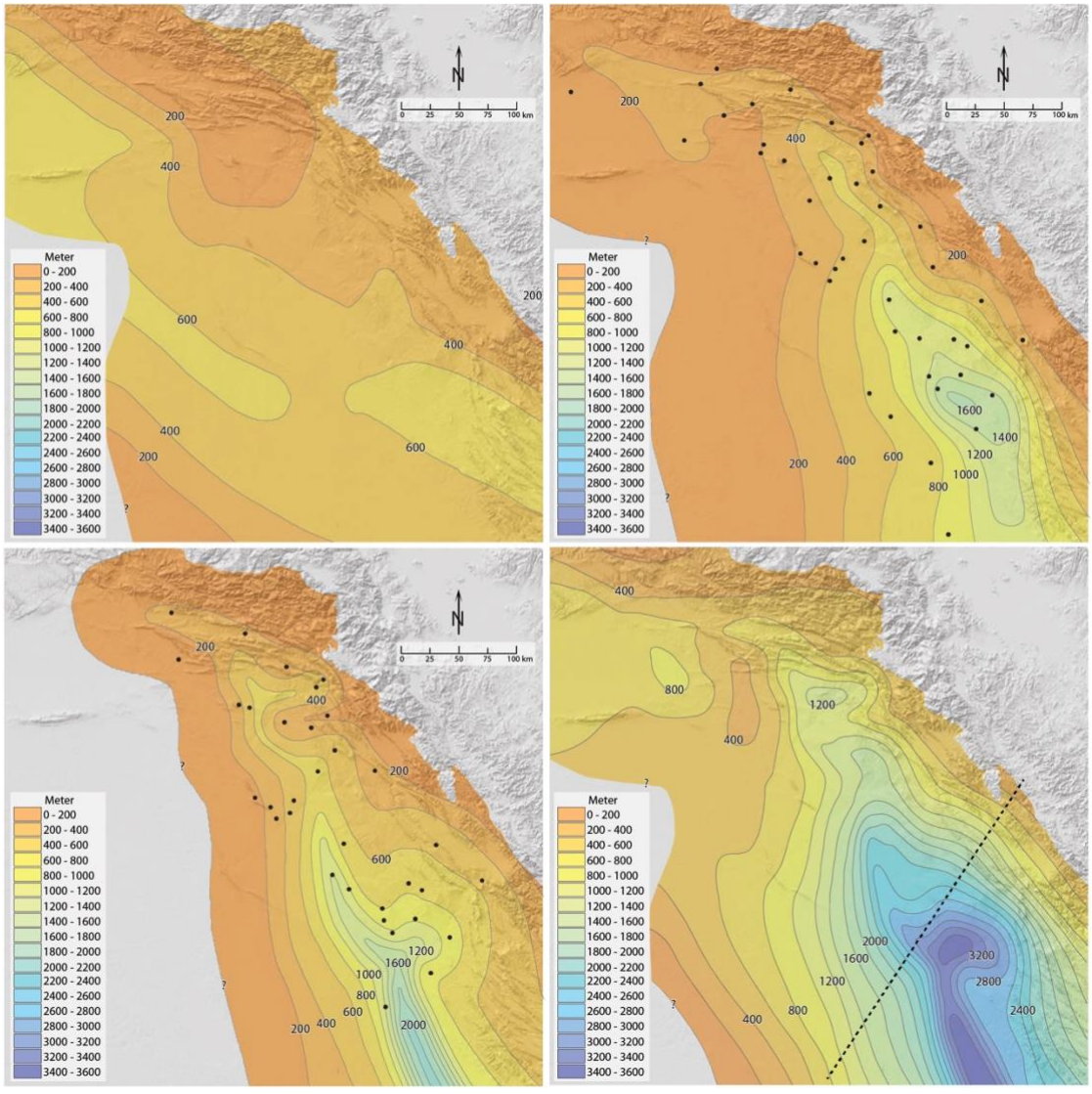

Figure 3: Isopach maps for the period ~15-5 Ma illustrating the thickness and depozone's distribution for the Fatha (a), Injana (b), Mukdadiya (c) Formations, and all together (d). Note the basin geometry change after the deposition of the Fatha Formation (middle Miocene). Black dots represent control points used to construct the contour lines. The Fatha Formation isopach map is based mainly on Dunnington (1958).

https://doi.org/10.5194/egusphere-2023-3123
Preprint. Discussion started: 24 January 2024

4.2 Subsidence curves and forward modeling of the flexural profile

The subsidence curves obtained from backstripping (see the yellow stars in Figure 2 for location of curves) show an overall convex-up shape, which is mainly characterized by rapid tectonic subsidence after ~20 Ma (Fig. 4), consistent with other examples of foreland basin subsidence curves (e.g., Xie and Heller, 2009). Flexural modeling of the Neogene Zagros tectonic and sedimentary loads (Fig. 5) demonstrates that both loads produce a shallower accommodation than we observed for the Neogene basin (base of Fatha Formation).

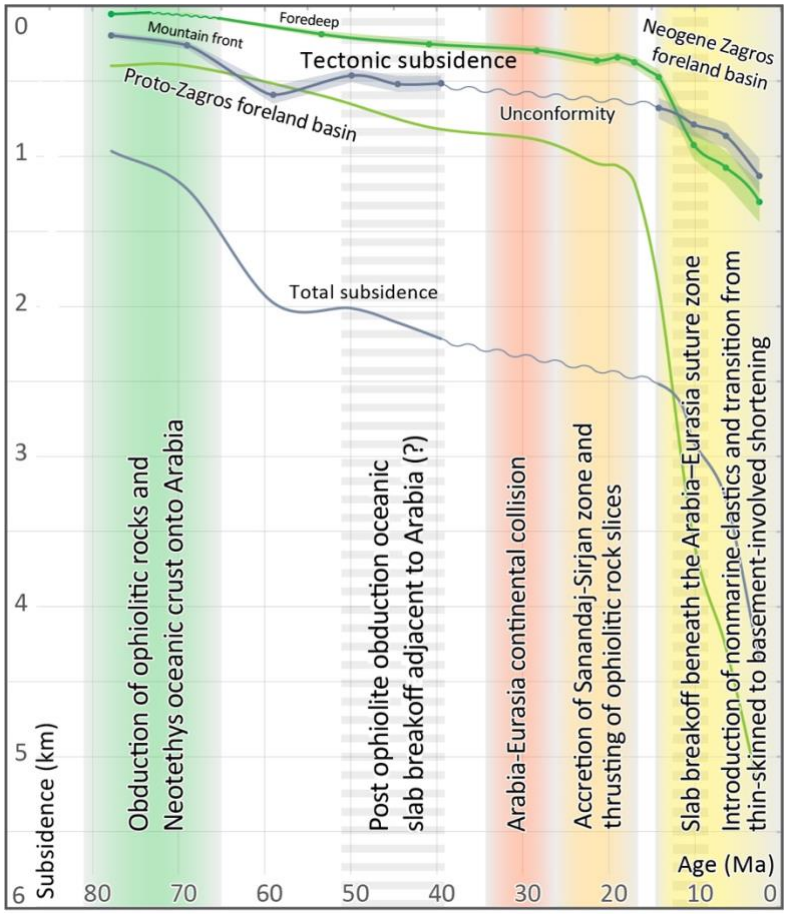

Figure 4: Subsidence analysis for two locations (mountain front in purple and foredeep in green; see estimated locations in Fig. 3d) showing tectonic and total subsidence. The shaded color of the tectonic subsidence curves depicts a 10% error. Colored and grey dashed bars represent major tectonic events in the geologic record of northeastern Arabia.

https://doi.org/10.5194/egusphere-2023-3123
Preprint. Discussion started: 24 January 2024

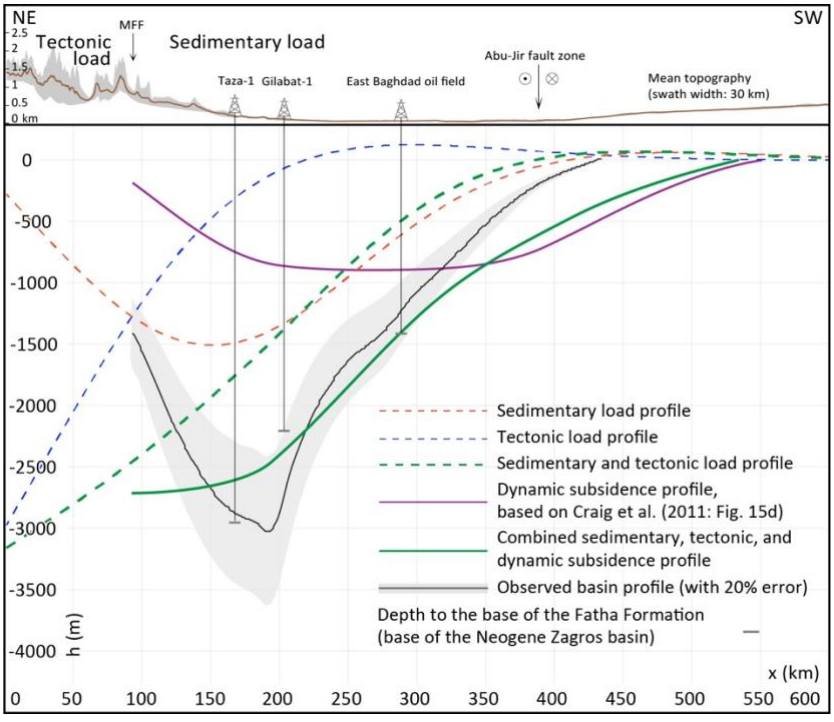

Figure 5: Modeled flexural profiles due to sedimentary and tectonic loads, and both loads together, as well as their combination with the dynamic subsidence profile in comparison to the observed basin flexure across the southeastern segment of the study area (see the trace line in Fig. 2b). Dynamic subsidence curve is based on the dynamic topography map of Craig et al. (2011: Fig. 15d). The observed basin profile is the arithmetic summation of the constructed isopach maps. MFF–mountain front flexure.

For the northeastern part of the basin near the MFF (Fig. 2), the subsidence curve exhibits a convex-up shape between ~80-60 Ma and later after ~40 Ma, followed by a ~25 Ma unconformity (Fig. 4: the grey curve labeled as mountain front). The southern subsidence curve (Fig. 4: the green curve labeled as foredeep) involves an unconformity between ~72 and 60 Ma, and shows slow subsidence for most of the Paleogene. Overall, the tectonic load is responsible for ~1100-1300 m subsidence in the NW Zagros belt (Figure 5), and the tectonic load alone could produce a deflection as deep as ~1387 m near the mountain front flexure (MFF), which is comparable to the tectonic subsidence resulting from backstripping (Fig. 4). Near the MFF, the combined tectonic and sedimentary loads lead to ~2560 m of subsidence, yet in the depocenter of the basin, where the observed depth is ~3000 m, the predicted deflection depth due to tectonic and sedimentary loads is only ~1629 m. Accordingly, the modeled basin subsidence from tectonic and sedimentary loads is markedly less than the total

https://doi.org/10.5194/egusphere-2023-3123
Preprint. Discussion started: 24 January 2024

accommodation that was generated in the basin since the middle Miocene when the deposition of the Fatha Formation commenced.

4.3 Bouguer gravity anomaly, dynamic topography, and tomography maps

The observed regional Bouguer gravity anomaly in the NW Zagros fold-thrust belt and foreland basin highlights a notable difference between the NE/E and the SW/W (Fig. 6a). In this sense, the overall negative gravity values in the NE/E may represent a deeper basin and the gravity signal of a crustal root beneath the belt. In the dynamic topography map (Fig. 6b), the positive values point towards uplift along the Arabia–Eurasia suture zone in the NE/E and most of the northeastern fold-thrust belt area. In contrast, the foreland basin part is dominated by subsidence, which reaches ~800 m in the south. Moreover, the present-day spatial organization of the Tigris and its tributaries, overall, coincides with the dynamic topography variation, but locally, it is more influenced by basement strike-slip faults, where the Bouguer gravity anomaly values show changes.

The tomographic map (200 km depth slice) of the Middle East (Fig. 7a) and the tomographic profiles across the NW Zagros fold-thrust belt and foreland basin (Fig. 7b) show the occurrence of a N-S-oriented zone of a low seismic velocity (presumably hot material with a lower density) anomaly in western Arabia and eastern Turkey, and distribution of fast velocity (high-density cold material) anomalies beneath the NW Zagros belt (Fig. 7a,b). The tomographic profiles I, II, and III (Fig. 7b) indicate that low-density hot material dominates the upper ~400 km of the upper Mantle in northern Arabia and eastern Turkey, whereas farther southward, high-density cold material is prominent throughout the upper mantle. Furthermore, the crystallization age of mantle magmatism since the late Eocene (Ball et al., 2021) plotted on the tomography maps shows a spatial correlation with the distribution of the low seismic velocity hot mantle material (Fig. 7c).

5 Discussion

5.1 Flexural subsidence in the NW Zagros foreland basin

Lines of evidence from this study reveal basin genesis as a flexural foreland basin that was later, during the late Miocene, influenced by dynamic topography due to slab tearing in the NW and northward mantle flow.

https://doi.org/10.5194/egusphere-2023-3123
Preprint. Discussion started: 24 January 2024

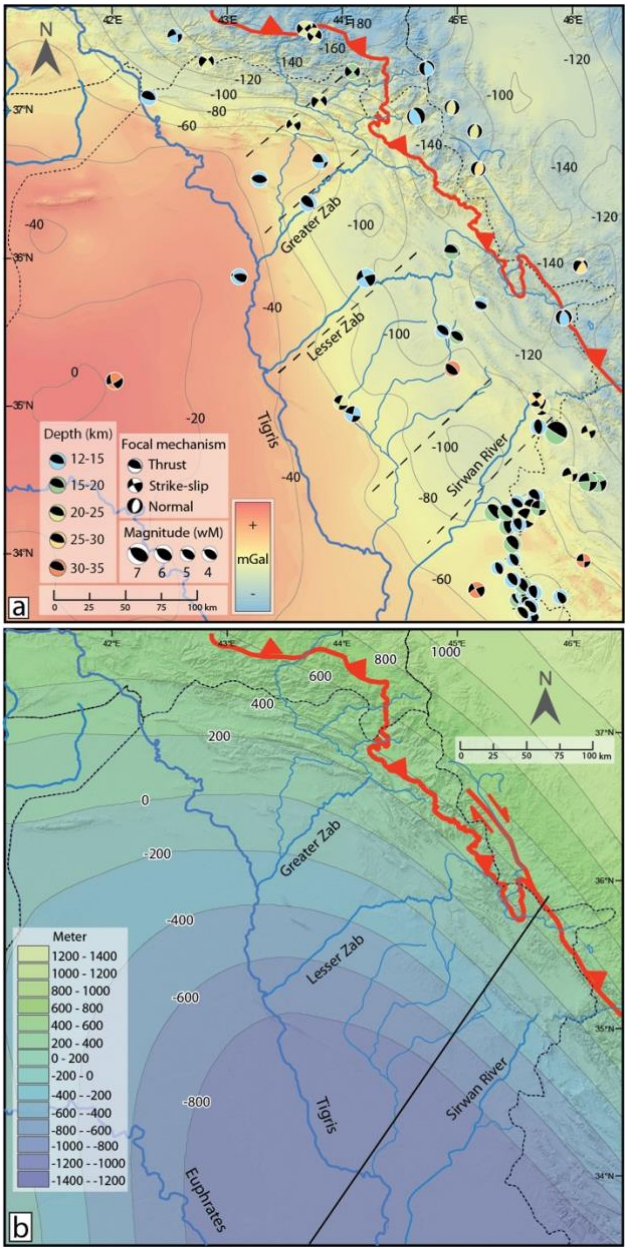

230

Figure 6: (a) Regional Bouguer gravity anomaly map with a spatial resolution of 2.5 arc-minute by 2.5 arc-minute (EGM2008: Pavlis et al., 2008) for the NW Zagros fold-thrust belt and foreland basin, showing low values in the northeastern segment. (b) Dynamic topography map of the NW Zagros fold-thrust belt and foreland basin that digitized from the published map of Craig et al. (2011: Fig. 15d).

https://doi.org/10.5194/egusphere-2023-3123
Preprint. Discussion started: 24 January 2024

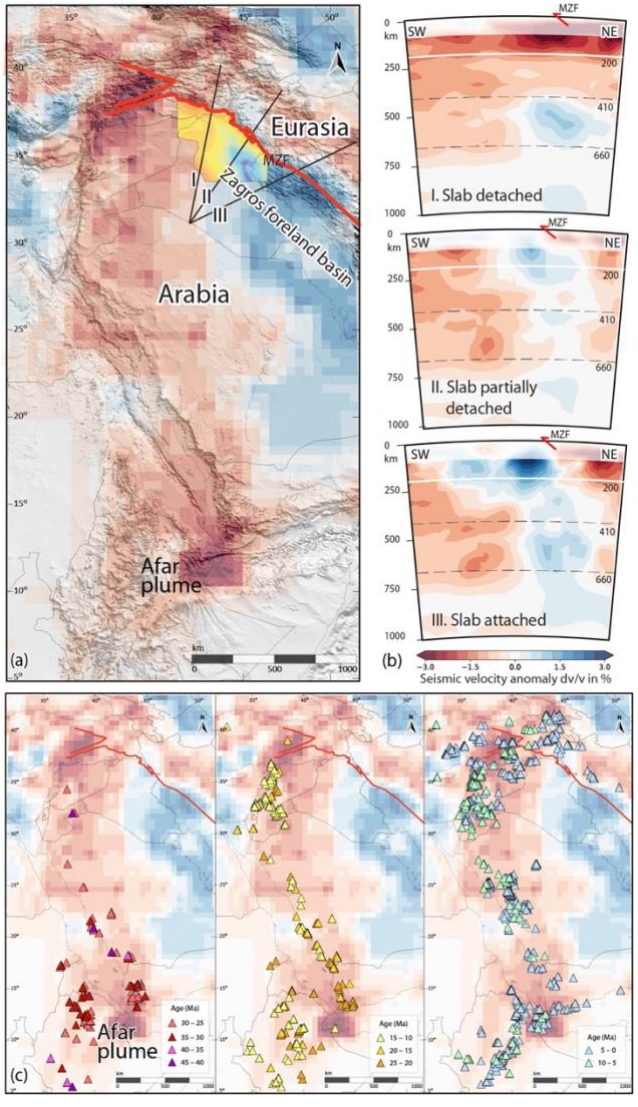

Figure 7: (a) Neogene deposits' isopach map (~15-5 Ma) of the NW Zagros foreland basin posted on the tomographic and shaded relief maps, illustrating that the basin depocenter is where the high-density cold upper mantle material is and vice-versa. (b) Tomographic cross-section across lines I, II, and III (a) across the NW Zagros fold-thrust belt and foreland basin. From top to bottom (NW to SE), the northeasterly vergence subducted high-velocity slab shows detachment to attachment. MZF–Main Zagros fault. (c) Tomographic map slices at 200 km depth of the Middle East based on the global P-wave velocity anomaly model UU-P07 (Amaru, 2007; Hall and Spakman, 2015) constructed by using SubMachine (Hosseini et al., 2018). From left to right, based on the crystallization age of mantle magmatism (Ball et al., 2021), magmatic rocks are subdivided into 45-25 Ma, 25-10 Ma, and 10-5 Ma and plotted on the tomographic map. The spatial distribution of magmatism through time in harmony with the upper mantle longitudinal N-S slow seismic velocity (low-density hot material) highlights the influence of the Afar plume generation and northward flow.

https://doi.org/10.5194/egusphere-2023-3123
Preprint. Discussion started: 24 January 2024

As presented in the flexural modeling result section, the present-day topography cannot produce a basin flexure as deep as the observed depth. The shift in stratal thicknesses, displayed by the isopach maps since the deposition of the Fatha Formation, indicates that the basin continuously subsided in the southern part of the study area. In contrast, the northern and northwestern parts experienced reduced accommodation during the deposition of the Injana, Mukdadiya, and Bai-Hasan Formations. During the early-middle Miocene, when the Fatha Formation was deposited, flexural bending due to the combined effect of topographic and slab loads was the primary mechanism for driving the subsidence of the Arabian foreland plate. We infer that these mechanisms were at work because of the NW–SE trending paleotopography of the proto-Zagros fold-thrust belt, forming a topographic load, and the subduction of the Arabian plate, resulting in a bending component due to slab load. Afterward, the NW Zagros foreland basin differentially subsided, resulting in a deep basin in the southern part. The incompatibility between observed and predicted flexural profiles was also proposed by Saura et al. (2015). However, another flexural profile model (Pirouz et al., 2017) predicts that the observed basin profile is shallower in the NW Zagros belt, contrary to the presented model in this study. Such inconsistency could be related to the fact that the latter model (1) considered the top of the Asmari Formation as the base of the foreland basin, and (2) the topographic load limit extended beyond the Arabia-Eurasia suture. In this study, the base of the Fatha Formation was considered as the base of the foreland basin based on subsidence curve analysis (Fig. 4), and the drainage divide, which spatially coincides with the MZF, was considered as the limit of the topographic load (Sinclair and Naylor, 2012).

The results of provenance synthesis on the basis of detrital zircon U-Pb ages (Koshnaw et al., 2020b: Fig. 10) from the Injana to the Mukdadiya Formations show a noticeable increase in the Paleogene age component (from ~20% to ~50%), pointing to a sediment source situated in the eastern terranes. Conversely, the Paleozoic age components mainly sourced from the northern terranes decreased (from ~50% to ~30%). Such provenance change suggests an earlier uplift in the northern terranes compared to the eastern terranes. Additionally, the isopach map of the Injana Formation hints at an orogen-parallel river system (Fig. 3b), whereas the Mukdadiya Formation isopach map points to sediment input from an orogen-perpendicular river into the existing orogen-parallel system (Fig. 3c), in line with results from provenance data. This inference is also consistent with the synthesis of the drainage network evolution in the Euphrates and Tigris River basin

https://doi.org/10.5194/egusphere-2023-3123
Preprint. Discussion started: 24 January 2024

(Wilson et al., 2014; McNab et al., 2017), which point to the occurrence of an earlier topographic growth in the northern terranes rather than in the South or southeastern segments of the Zagros orogen. Accordingly, provenance data paired with source area topographic growth history suggest that terrane uplift occurred first in the north while the basin rapidly subsided in the south. Therefore, flexural subsidence alone is unlikely to explain the deep basin in the southern part of the study area, and an additional driver is necessary.

5.2. Dynamic subsidence and Afar plume northward flow

Dynamic subsidence in combination with flexure subsidence could be invoked to conjointly account for the observed ~3-4 km thick accommodation in the southeastern segment of the basin (Fig. 5). Deep earth processes such as horizontal slab tearing beneath the northwestern segment of the Arabia-Eurasia suture zone and Afar mantle plume flow above the detached segment could be linked to the localization of the basin subsidence in the NW Zagros.

Slab-pull force is a crucial driving force for plate motion, and it is altered by slab tearing and detachment (Wortel and Spakman, 2000). In regions where the slab is detached, the slab-pull force no longer impacts the surface above the detachment, but instead, the force intensifies on the still attached part of the slab. This change in force balance results in an enhanced downward tension on the tearing tip and lateral propagation of detachment. The surface region above the detached segment of the slab undergoes uplift, whereas the area above the still attached slab experiences subsidence (van der Meulen et al., 1998; Wortel and Spakman, 2000). These predictions are observed in the geology of the NW Zagros basin.

Tectonic subsidence curves constrain the onset of foreland basin subsidence to the timing of Fatha Formation deposition. The reported depositional time of the Fatha Formation spans from the early to middle Miocene based on fossil content and $^{87}Sr/^{86}Sr$ isotope chronostratigraphy (Al-Naqib, 1959; Mahdi, 2007; Grabowski and Liu, 2010; Hawramy and Khalaf, 2013). Later during the deposition of the Injana Formation during ~12.4-8 Ma (based on magnetostratigraphy: Koshnaw et al., 2020b), the basin underwent rapid subsidence in the SE, but the NW segment experienced limited accommodation genesis (Figs. 3). Furthermore, the Bouguer gravity anomaly map suggests a remarkable difference in basement depth between the northeast and the southeast of the NW Zagros belt (Fig. 6a). This variation of depth was interpreted to be as shallow as ~5-6 km in the west and as deep as ~12 km in the east (Konert et al., 2001). The shallower depth-to-basement in the western part of the NW Zagros belt may also be related to the basement paleotopographic variation. In the NW and W Iraq, paleohighs with reduced sedimentation have been suggested for periods even before the Miocene (Jassim and Buday, 2006). However, considering how consistent is the isopach map of the Fatha Formation throughout the west to the east, potential paleohighs seem to have had limited or no influence on the low accommodation during the deposition of the post-Fatha formations. We argue that this variation of the basin subsidence in the east versus west is linked to the slab tearing and dynamic subsidence.

https://doi.org/10.5194/egusphere-2023-3123
Preprint. Discussion started: 24 January 2024

Dynamic subsidence dominates the area in the NW Zagros belt (Fig. 6b). It deflects the southeastern segment of the basin up to ~800 m, as estimated from free-air gravity anomaly (Craig et al., 2011). Combining the dynamic subsidence amount with the subsidence amount due to surface load successfully reproduces the observed ~3-4 km deep Neogene basin in the S/SE (Figs. 5), arguing for mantle influence (Fig. 7). The lithospheric process of horizontal slab tear actively induces and reorders mantle flow, leading to long wavelength surface topographic variation (Dávila and Lithgow-Bertelloni, 2013; Faccenna et al., 2013). In the northern Middle East, Neotethys oceanic slab detachment and hot mantle material emplacement at shallow depth have been suggested between the Arabian and Eurasian plates and beneath the Turkish–Iranian plateau (TIP) on the basis of geochemical data and seismic tomography (Keskin, 2003; Hafkenscheid et al., 2006; Omrani et al., 2008; Koulakov et al., 2012; Kaviani et al., 2018). On the surface (Figs. 7a,b), lateral migration of detachment and the associated shift in the mantle flow are manifested by uplift where the slab is detached due to rebounding and hot mantle material replacement and further subsidence where it is still attached due to slab weight and downward mantle material flow. Moreover, the spatial distribution of mantle magmatism since ~45 Ma and its concurrence with the Afar plume northward flow (Camp and Roobol, 1992; Ershov and Nikishin, 2004; Faccenna et al., 2013) are suggestive of a pre ~10 Ma slab detachment. This is because of mantle magmatism distribution beyond the Arabia-Eurasia suture zone only after ~10 Ma (Figs. 7c, 8). The early development of the Afar mantle material northward flow and its arrival at the Arabia-Eurasia suture zone by the middle to late Miocene possibly contributed to the slab tearing initiation, particularly in the western where the Arabian continental curt transition into the oceanic crust in the Mediterranean region. The effect of mantle flowing northward from the Afar plume has also been interpreted to drive the inversion of the right-lateral Abu-Jir fault zone during the early to middle Miocene in western Iraq, away from the ongoing Zagros-related shortening in the east (Alhadithi et al., 2023). The Afar mantle material northward flow is further supported by mantle transition zone thickness anomaly (Kaviani et al., 2018) and fast velocity polarization orientation analysis (SKS splitting) (Faccenna et al., 2013). Furthermore, the Afar plume northward flow may also have influenced the Mediterranean tectonic history and fostered the Arabia-Eurasia convergence (~3-2 cm/yr), even after the Oligocene continental collision (Jolivet and Faccenna, 2000; Alvarez et al., 2010; Boutoux et al., 2021) (Fig. 9).

In brief, these lines of evidence argue for the NW Zagros foreland basin transitioning from a flexural foreland basin to a mantle–influenced basin due to slab tearing during the late Miocene (Fig. 10), which enhanced and localized subsidence in the southeast of the basin.

https://doi.org/10.5194/egusphere-2023-3123
Preprint. Discussion started: 24 January 2024

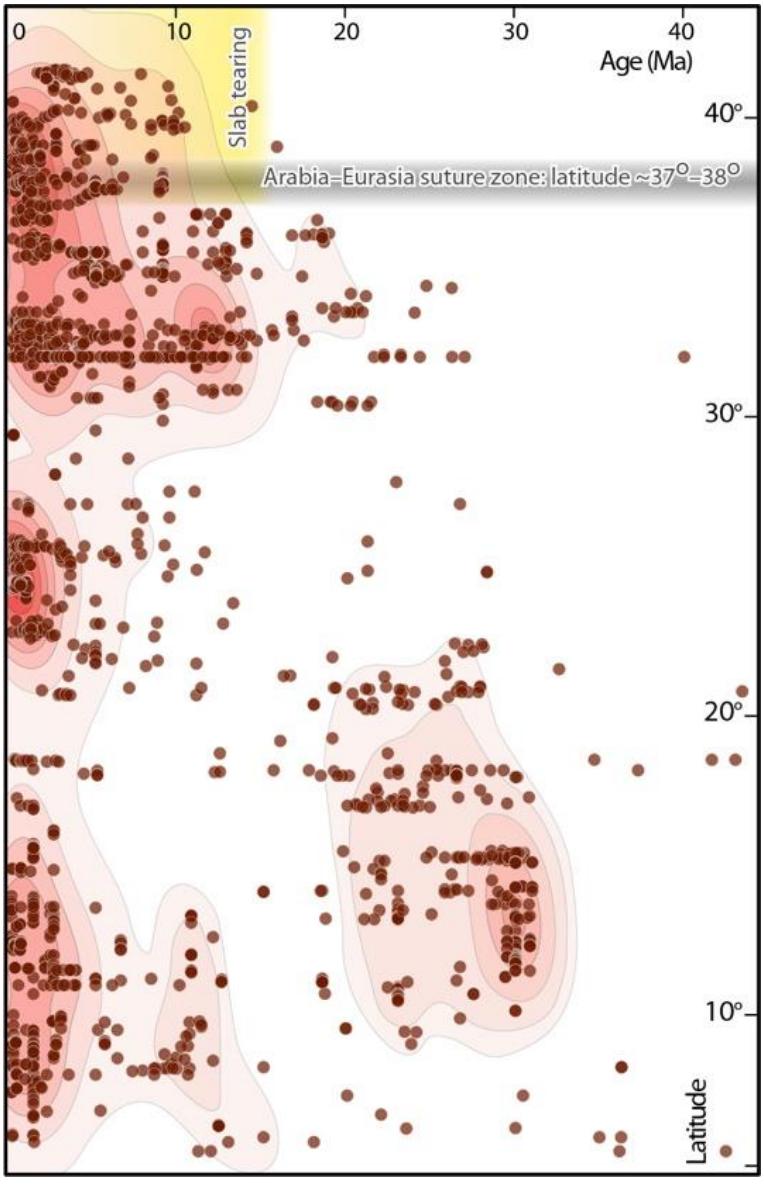

335

Figure 8: Mantle-related magmatic rock age versus latitude plotted as bivariate kernel density estimation showing intense magmatism beyond the Arabia-Eurasia suture zone in the Turkish-Iranian plateau after ~10 Ma. Magmatic age data are from Ball et al. (2021).

340

https://doi.org/10.5194/egusphere-2023-3123
Preprint. Discussion started: 24 January 2024

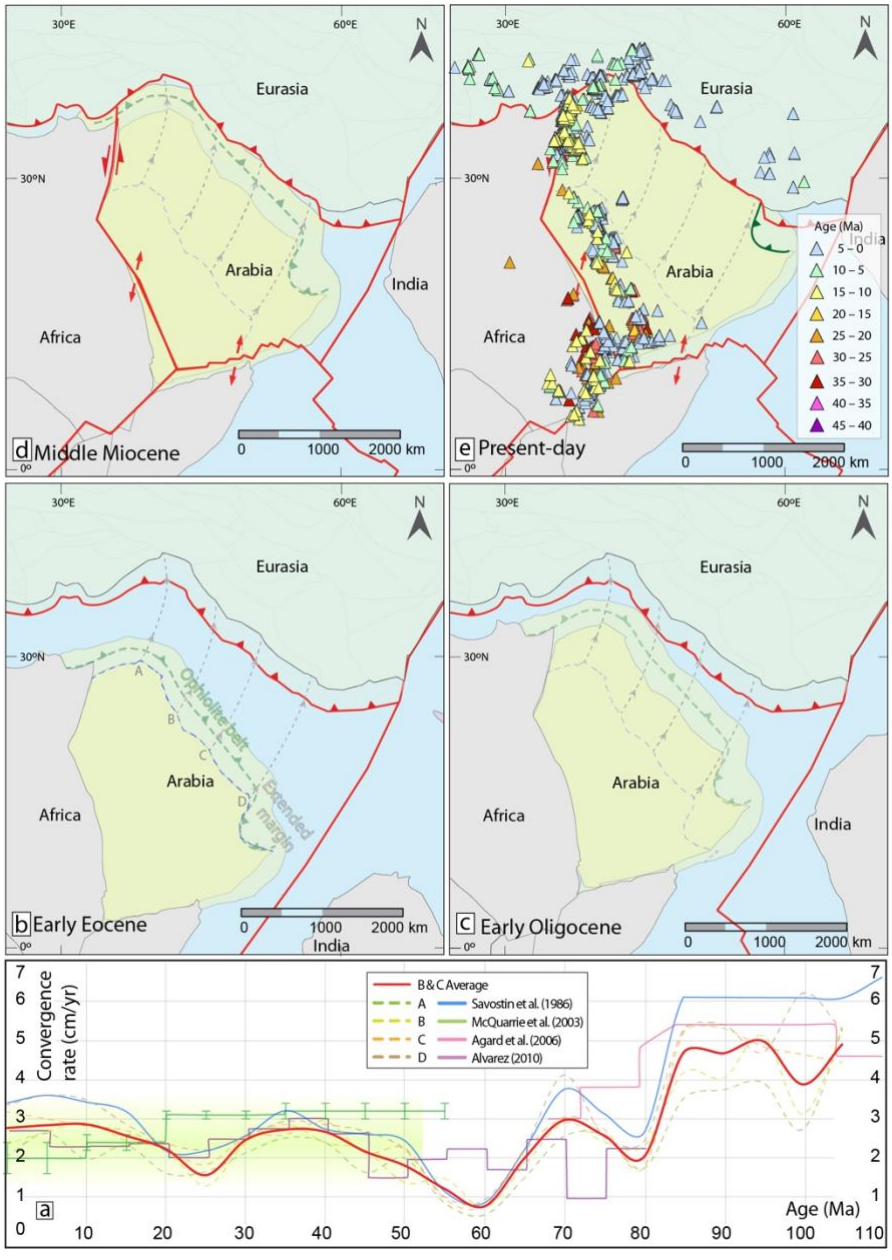

Figure 9: (a) Convergence rate between moving Arabia against fixed Eurasia calculated from reference points (A, B, C, and D) from the Arabian plate based on plate kinematic reconstruction of Müller et al. (2018; GPlates 2.2.0) and compared with other published convergence rate (Savostin et al., 1986; McQuarrie et al., 2003; Agard et al., 2006; Alvarez et al., 2010). (b-e) The Arabian plate kinematic reconstruction with respect to the fixed Eurasia since the early Eocene (~55 Ma) is based on Müller et al. (2018). The width of the Eurasian outer margin during Paleogene is estimated from the present-day width of the Makran accretionary wedge (~500-300 km; e.g., Burg et al. 2018).

https://doi.org/10.5194/egusphere-2023-3123
Preprint. Discussion started: 24 January 2024

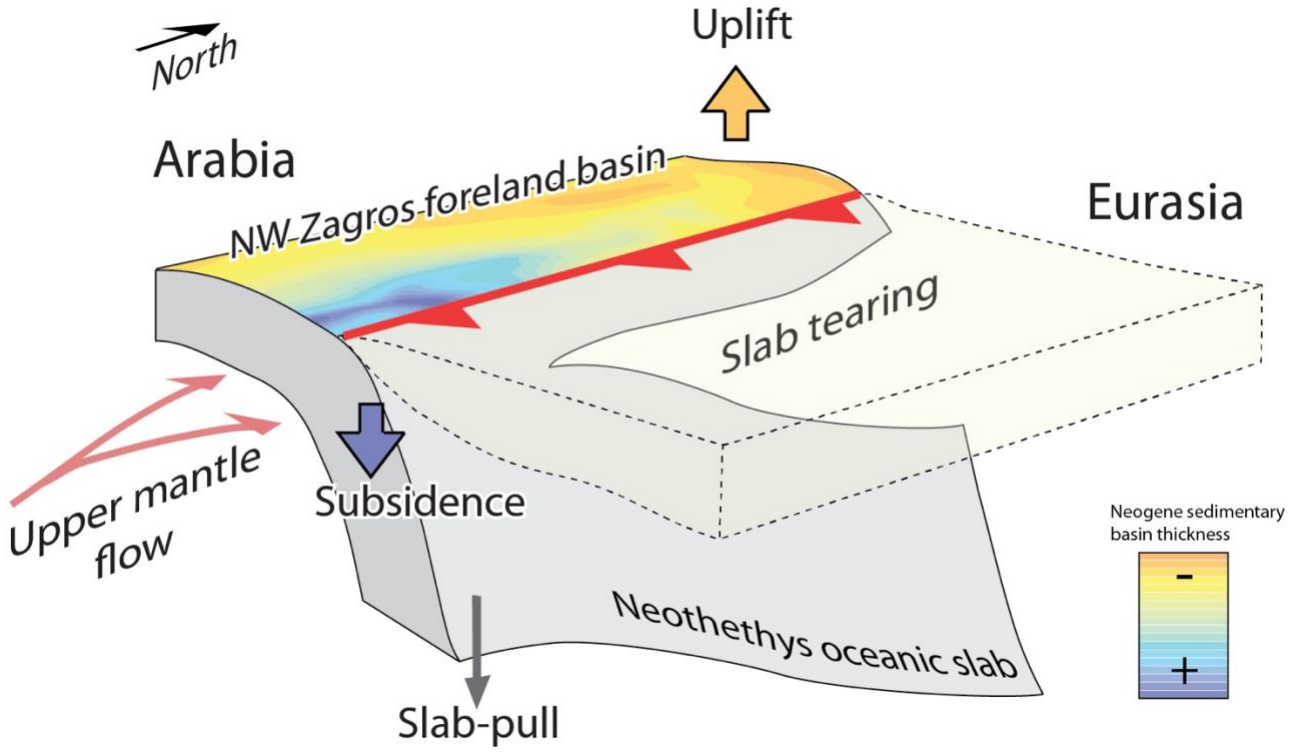

350

Figure 10: Conceptual illustration portraying the NW Zagros foreland basin evolution during Neogene in response to the downgoing Neotethys oceanic slab tearing, detachment, and breakoff along the Arabia-Eurasia suture zone from the NW to the SE, and upper mantle material northward flow in western Arabia.

6 Conclusions

355 Isopach maps for the middle and upper Miocene formation in the NW Zagros Foreland basin reveal continuous subsidence in the southeastern part, while the northwestern segment had limited accommodation. In its southeastern segment, the Neogene Zagros foreland basin thickens to ~4 km, incompatible with the adjacent moderate mountain topography (~1.5-2.5 km). We invoke a substantial contribution of dynamic subsidence to explain the abnormally high accommodation space in the southern segment of the basin. Lines of evidence from this study argue that the NW Zagros foreland basin underwent a two-
360 stage basin evolution: (1) an early basin flexure due to surface and slab loads during the early to middle Miocene, and (2) a later stage when the basin was modified by the propagation of the Neotethys horizontal slab-tear from the northwest to the southeast. In other words, the present-day deep basin resulted from flexural subsidence and dynamic subsidence. Due to the SE-ward Neotethys oceanic crust slab tear, the Afar mantle plume propagated beneath the TIP and beyond the Arabia and Eurasia suture zone in the NW. Based on the timing of mantle magmatism and their spatial distribution beyond the suture

https://doi.org/10.5194/egusphere-2023-3123
Preprint. Discussion started: 24 January 2024

zone in the NW and concordant with hot mantle dissemination, as well as the timing of the shift in basin architecture, the slab tear is expected to have taken place during the late Miocene. This study demonstrates the coexistence of flexural and dynamic subsidence in the NW Zagros foreland basin, emphasizing the importance of slab tearing and mantle dynamics in shaping the basin's architecture after the collision.

Data availability. The data used in this article will be available at Mendeley Data repository and are already available to the reviewers.

Supplement.

Author contributions. RK: leadership responsibility, funding acquisition, conceptualization, data curation, formal analyses, investigation, visualization, and writing (original draft preparation). Jonas Kley: resources, conceptualization, and writing (review and editing). FS: conceptualization and writing (review and editing).

Competing interests. The authors declare that they have no known competing financial interests or personal relationships that could have appeared to influence the work reported in this paper.

Disclaimer. Publisher's note: Copernicus Publications remains neutral with regard to jurisdictional claims in published maps and institutional affiliations.

Acknowledgments. The first author, R. I. Koshnaw, benefited from discussions with M. Zebari, M. Tamar-Agha, M. Kloecking, and M. Correa. This work was fully supported by the Alexander von Humboldt research fellowship awarded to R. I. Koshnaw.

Financial support. This work was fully supported by the Alexander von Humboldt research fellowship awarded to R. I. Koshnaw.

Review statement.

https://doi.org/10.5194/egusphere-2023-3123
Preprint. Discussion started: 24 January 2024

References

Agard, P., Monié, P., Gerber, W., Omrani, J., Molinaro, M., Meyer, B., ... & Yamato, P.: Transient, synobduction exhumation of Zagros blueschists inferred from P-T, deformation, time, and kinematic constraints: Implications for Neotethyan wedge dynamics. Journal of Geophysical Research: Solid Earth, 111(B11), 2006.

Al-Hadithi, A.K.A., Fajer, R.N. and Koshnaw, R.I.: Early-middle Miocene Inversion of the Abu Jir Fault in the Western Iraq: a Possible Consequence of the Arabian Plate Northward Movement. The Iraqi Geological Journal, 247-259, 2023.

Al-Naqib, K.M.: Geology of the Southern area of Kirkuk Liwa, Iraq". IPC. Technical pub. London, internal report, 1959.

Al-Sheikhly, S.S., Tamar-Agha, M.Y. and Mahdi, M.M.: Basin analysis of Cretaceous to Tertiary selected wells in Kirkuk and Bai Hassan Oil Fields, Kirkuk, Northern Iraq. Iraqi Journal of Science, 56(1B), 435-443, 2015.

Allen, M.B. and Armstrong, H.A.: Arabia–Eurasia collision and the forcing of mid-Cenozoic global cooling. Palaeogeography, Palaeoclimatology, Palaeoecology, 265(1-2), 52-58, 2008.

Allen, P.A. and Allen, J.R.: Basin analysis: Principles and application to petroleum play assessment, John Wiley & Sons, 2013.

Alvarez, W.: Protracted continental collisions argue for continental plates driven by basal traction. Earth and Planetary Science Letters, 296(3-4), 434-442, 2010.

Amaru, M.: Global travel time tomography with 3-D reference models, Geol. Traiectina (Doctoral dissertation, PhD thesis, Utrecht Univ. 1–174), 2007.

Angevine, C.L., Heller, P.L. and Paola, C.: Quantitative sedimentary basin modeling, 1990.

ASTER Global Digital Elevation Map v.2.: METI and NASA, (accessed August 21, 2019), asterweb.jpl.nasa.gov/gdem.asp, 2011.

Balázs, A., Faccenna, C., Ueda, K., Funiciello, F., Boutoux, A., Blanc, E.J.P. and Gerya, T.: Oblique subduction and mantle flow control on upper plate deformation: 3D geodynamic modeling. Earth and Planetary Science Letters, 569, 117056, 2021.

Ball, P.W., White, N.J., Maclennan, J. and Stephenson, S.N.: Global influence of mantle temperature and plate thickness on intraplate volcanism. Nature Communications, 12(1), 2045, 2021.

Bodine, J.H., Steckler, M.S. and Watts, A.B.: Observations of flexure and the rheology of the oceanic lithosphere. Journal of Geophysical Research: Solid Earth, 86(B5), 3695-3707, 1981.

Boutoux, A., Briaud, A., Faccenna, C., Ballato, P., Rossetti, F. and Blanc, E.: Slab folding and surface deformation of the Iran mobile belt. Tectonics, 40(6), p.e2020TC006300, 2021.

Burg, J. P.: Geology of the onshore Makran accretionary wedge: Synthesis and tectonic interpretation. Earth-Science Reviews, 185, 1210-1231, 2018.

Camp, V. E., & Roobol, M. J.: Upwelling asthenosphere beneath western Arabia and its regional implications. Journal of Geophysical Research: Solid Earth, 97(B11), 15255-15271, 1992.

https://doi.org/10.5194/egusphere-2023-3123
Preprint. Discussion started: 24 January 2024

Cardozo, N.: Flex2D. https://www.ux.uis.no/~nestor/work/programs.html, 2021.

Conrad, C.P. and Lithgow-Bertelloni, C.: The temporal evolution of plate driving forces: Importance of "slab suction" versus "slab pull" during the Cenozoic. Journal of Geophysical Research: Solid Earth, 109(B10), 2004.

Craig, T.J., Jackson, J.A., Priestley, K. and McKenzie, D.: Earthquake distribution patterns in Africa: their relationship to variations in lithospheric and geological structure, and their rheological implications. Geophysical Journal International, 185(1), 403-434, 2011.

Davies, J.H. and von Blanckenburg, F.: Slab breakoff: a model of lithosphere detachment and its test in the magmatism and deformation of collisional orogens. Earth and planetary science letters, 129(1-4), 85-102, 1995.

Dávila, F.M. and Lithgow-Bertelloni, C.: Dynamic topography in South America. Journal of South American Earth Sciences, 43, 127-144, 2013.

DeCelles, P.G., 2012. Foreland basin systems revisited: Variations in response to tectonic settings. Tectonics of sedimentary basins: Recent advances, 405-426.

Dunnington, H.V.: Generation, migration, accumulation, and dissipation of oil in northern Iraq: Middle East, 1958.

Duretz, T. and Gerya, T.V.: Slab detachment during continental collision: Influence of crustal rheology and interaction with lithospheric delamination. Tectonophysics, 602, 124-140, 2013.

English, J.M., Lunn, G.A., Ferreira, L. and Yacu, G.: Geologic evolution of the Iraqi Zagros, and its influence on the distribution of hydrocarbons in the Kurdistan region. AAPG Bulletin, 99(2), 231-272, 2015.

Ershov, A. V., & Nikishin, A. M.: Recent geodynamics of the Caucasus-Arabia-east Africa region. Geotectonics, 38(2), 123-136, 2004.

Faccenna, C., Becker, T. W., Jolivet, L., & Keskin, M.: Mantle convection in the Middle East: Reconciling Afar upwelling, Arabia indentation and Aegean trench rollback. Earth and Planetary Science Letters, 375, 254-269, 2013.

Faccenna, C., Becker, T.W., Holt, A.F. and Brun, J.P.: Mountain building, mantle convection, and supercontinents: revisited. Earth and Planetary Science Letters, 564, 116905, 2021.

Garefalakis, P. and Schlunegger, F.: Link between concentrations of sediment flux and deep crustal processes beneath the European Alps. Scientific Reports, 8(1),1-11, 2018.

Garzanti, E., Radeff, G. and Malusà, M.G.: Slab breakoff: A critical appraisal of a geological theory as applied in space and time. Earth-Science Reviews, 177, 303-319, 2018.

Grabowski, G.J. and Liu, C.: Strontium-isotope age dating and correlation of Phanerozoic anhydrites and unfossiliferous limestones of Arabia. In GEO 2010 (pp. cp-248). European Association of Geoscientists & Engineers, 2010.

Hafkenscheid, E., Wortel, M.J.R. and Spakman, W.: Subduction history of the Tethyan region derived from seismic tomography and tectonic reconstructions. Journal of Geophysical Research: Solid Earth, 111(B8), 2006.

Hall, R. and Spakman, W.: Mantle structure and tectonic history of SE Asia. Tectonophysics, 658, 14-45, 2015.

Hatzfeld, D. and Molnar, P.: Comparisons of the kinematics and deep structures of the Zagros and Himalaya and of the Iranian and Tibetan plateaus and geodynamic implications. Reviews of Geophysics, 48(2), 2010.

https://doi.org/10.5194/egusphere-2023-3123
Preprint. Discussion started: 24 January 2024

Heller, P.L. and Liu, L.: Dynamic topography and vertical motion of the US Rocky Mountain region prior to and during the Laramide orogeny. Bulletin, 128(5-6), 973-988, 2016.

Hetenyi, M.: Beams on Elastic Foundations. University of Michigan Press, Ann Arbor, 1946.

Hosseini, K., Matthews, K.J., Sigloch, K., Shephard, G.E., Domeier, M. and Tsekhmistrenko, M.: SubMachine: Web-based tools for exploring seismic tomography and other models of Earth's deep interior. Geochemistry, Geophysics, Geosystems, 19(5), 1464-1483, 2018.

Iraqi Bull. Geol. Min. 3 (1), 41–53, 2007.

Jassim, S. Z., and Buday, T.: Units of the unstable shelf and the Zagros Suture. In S. Z. Jassim & J. C. Goff (Eds.), The geology of Iraq (pp. 45–56). Prague and Brno, Czech Republic: Dolin and Moravian Museum, 2006.

Jolivet, L., & Faccenna, C.: Mediterranean extension and the Africa-Eurasia collision. Tectonics, 19(6), 1095-1106, 2000.

Jolivet, L., Menant, A., Sternai, P., Rabillard, A., Arbaret, L., Augier, R., ... & Le Pourhiet, L.: The geological signature of a slab tear below the Aegean. Tectonophysics, 659, 166-182, 2015.

Kaviani, A., Sandvol, E., Moradi, A., Rümpker, G., Tang, Z. and Mai, P.M.: Mantle transition zone thickness beneath the Middle East: Evidence for segmented Tethyan slabs, delaminated lithosphere, and lower mantle upwelling. Journal of Geophysical Research: Solid Earth, 123(6), 4886-4905, 2018.

Kennett, B.L.N., Engdahl, E.R., Buland, R.: Constraints on seismic velocities in the Earth from travel times. Geophys. J. Int. 122, 108–124, 1995.

Keskin, M., 2003. Magma generation by slab steepening and breakoff beneath a subduction-accretion complex: An alternative model for collision-related volcanism in Eastern Anatolia, Turkey. Geophysical Research Letters, 30(24).

Kissling, E. and Schlunegger, F.: Rollback orogeny model for the evolution of the Swiss Alps. Tectonics, 37(4), 1097-1115, 2018.

Konert, G., Afifi, A. M., Al-Hajri, S. I. A., & Droste, H. J.: Paleozoic stratigraphy and hydrocarbon habitat of the Arabian plate. GeoArabia, 6(3), 407–442, 2001.

Koshnaw, R.I., Horton, B.K., Stockli, D.F., Barber, D.E. and Tamar-Agha, M.Y.: Sediment routing in the Zagros foreland basin: Drainage reorganization and a shift from axial to transverse sediment dispersal in the Kurdistan region of Iraq. Basin Research, 32(4), 688-715, 2020b.

Koshnaw, R.I., Schlunegger, F. and Stockli, D.F.: Detrital zircon provenance record of the Zagros mountain building from the Neotethys obduction to the Arabia–Eurasia collision, NW Zagros fold–thrust belt, Kurdistan region of Iraq. Solid Earth, 12(11), 2479-2501, 2021.

Koshnaw, R.I., Stockli, D.F. and Schlunegger, F.: Timing of the Arabia-Eurasia continental collision—Evidence from detrital zircon U-Pb geochronology of the Red Bed Series strata of the northwest Zagros hinterland, Kurdistan region of Iraq. Geology, 47(1), 47-50, 2019.

https://doi.org/10.5194/egusphere-2023-3123
Preprint. Discussion started: 24 January 2024

Koshnaw, R.I., Stockli, D.F., Horton, B.K., Teixell, A., Barber, D.E. and Kendall, J.J.: Late Miocene deformation kinematics along the NW Zagros fold-thrust belt, Kurdistan region of Iraq: Constraints from apatite (U-Th)/He thermochronometry and balanced cross sections. Tectonics, 39(12), p.e2019TC005865, 2020a.

Koulakov, I., Zabelina, I., Amanatashvili, I. and Meskhia, V.: Nature of orogenesis and volcanism in the Caucasus region based on results of regional tomography. Solid Earth, 3(2), 327-337, 2012.

Kundu, B. and Santosh, M.: Dynamics of post-slab breakoff in convergent plate margins: a "jellyfish" model. American Journal of Science, 311(8), 701-717, 2011.

Mahdi, A.: Fossils Mollusca (bivalve) from the Fatha formation of northern Iraq.

McNab, F., Ball, P.W., Hoggard, M.J. and White, N.J.: Neogene uplift and magmatism of Anatolia: Insights from drainage analysis and basaltic geochemistry. Geochemistry, Geophysics, Geosystems, 19(1), 175-213, 2018.

McQuarrie, N. and van Hinsbergen, D.J.: Retrodeforming the Arabia-Eurasia collision zone: Age of collision versus magnitude of continental subduction. Geology, 41(3), 315-318, 2013.

McQuarrie, N., Stock, J. M., Verdel, C., & Wernicke, B. P.: Cenozoic evolution of Neotethys and implications for the causes of plate motions. Geophysical research letters, 30(20), 1986.

Müller, R. D., Cannon, J., Qin, X., Watson, R. J., Gurnis, M., Williams, S., ... & Zahirovic, S.: GPlates: Building a virtual Earth through deep time. Geochemistry, Geophysics, Geosystems, 19(7), 2243-2261, 2018.

Niu, Y.L.: Slab breakoff: a causal mechanism or pure convenience? Science bulletin., 62(7), 456-461, 2017.

Omrani, J., Agard, P., Whitechurch, H., Benoit, M., Prouteau, G. and Jolivet, L.: Arc-magmatism and subduction history beneath the Zagros Mountains, Iran: a new report of adakites and geodynamic consequences. Lithos, 106(3-4), 380-398, 2008.

Pavlis, N. K., S. A. Holmes, S. C. Kenyon, J. K. Factor. An Earth Gravitational Model to Degree 2160: EGM2008, EGU General Assembly 2008, Vienna, Austria, April 13-18, 2008.

Pirouz, M., Avouac, J.P., Gualandi, A., Hassanzadeh, J. and Sternai, P.: Flexural bending of the Zagros foreland basin. Geophysical Journal International, 210(3), 1659-1680, 2017.

Royden, L. and Faccenna, C.: Subduction orogeny and the Late Cenozoic evolution of the Mediterranean Arcs. Annual Review of Earth and Planetary Sciences, 46, 261-289, 2018.

Royden, L.H.: The tectonic expression slab pull at continental convergent boundaries. Tectonics, 12(2), 303-325, 1993.

Sachsenhofer, R.F., Bechtel, A., Gratzer, R. and Rainer, T.M.: Source-rock maturity, hydrocarbon potential, and oil–source-rock correlation in well shorish-1, Erbil province, Kurdistan region, Iraq. Journal of Petroleum Geology, 38(4), 357-381, 2015.

Saura, E., Garcia-Castellanos, D., Casciello, E., Parravano, V., Urruela, A. and Vergés, J.: Modeling the flexural evolution of the Amiran and Mesopotamian foreland basins of NW Zagros (Iran-Iraq). Tectonics, 34(3), 377-395, 2015.

Savostin, L. A., Sibuet, J. C., Zonenshain, L. P., Le Pichon, X., & Roulet, M. J.: Kinematic evolution of the Tethys belt from the Atlantic Ocean to the Pamirs since the Triassic. Tectonophysics, 123(1-4), 1-35, 1986.

https://doi.org/10.5194/egusphere-2023-3123
Preprint. Discussion started: 24 January 2024

Schlunegger, F. and Kissling, E.: Slab load controls beneath the Alps on the source-to-sink sedimentary pathways in the Molasse basin. Geosciences, 12(6), 226, 2022.

Schlunegger, F. and Kissling, E.: Slab rollback orogeny in the Alps and evolution of the Swiss Molasse basin. Nature communications, 6(1), 8605, 2015.

Shawkat, M.G. and Tucker, M.E.: Stromatolites and sabkha cycles from the Lower Fars Formation (Miocene) of Iraq. Geologische Rundschau, 67, 1-14, 1978.

Sinclair, H. D., & Naylor, M.: Foreland basin subsidence driven by topographic growth versus plate subduction. Bulletin, 124(3-4), 368-379, 2012.

Sinclair, H.D.: Flysch to molasse transition in peripheral foreland basins: The role of the passive margin versus slab breakoff. Geology, 25(12), 1123-1126, 1997.

Van der Meulen, M.J., Meulenkamp, J.E. and Wortel, M.J.R.: Lateral shifts of Apenninic foredeep depocentres reflecting detachment of subducted lithosphere. Earth and Planetary Science Letters, 154(1-4), 203-219, 1998.

van Hunen, J. and Allen, M.B.: Continental collision and slab break-off: A comparison of 3-D numerical models with observations. Earth and Planetary Science Letters, 302(1-2), 27-37, 2011.

Vanderhaeghe, O.: The thermal–mechanical evolution of crustal orogenic belts at convergent plate boundaries: A reappraisal of the orogenic cycle. Journal of Geodynamics, 56, 124-145, 2012.

Wilson, J.W.P., Roberts, G.G., Hoggard, M.J. and White, N.J.: Cenozoic epeirogeny of the A rabian P eninsula from drainage modeling. Geochemistry, Geophysics, Geosystems, 15(10), 3723-3761, 2014.

Wortel, M.J.R. and Spakman, W.: Subduction and slab detachment in the Mediterranean-Carpathian region. Science, 290(5498), 1910-1917, 2000.

Xie, X. and Heller, P.L.: Plate tectonics and basin subsidence history. Geological Society of America Bulletin, 121(1-2), 55-64, 2009.